A GPS Simulator for Analysis of Channel Impairments in Practical Scenarios

Cynthia Junqueira[1,2], Danilo Zanatta Filho[1]
João Batista Destro Filho[1] , Murilo B. Loiola[1] and João Marcos T. Romano[1]

[1]State University of Campinas (Unicamp), Campinas, Brazil
[2]AerospaceTechnical Center – Aeronautic and Space Institute, São José dos Campos, Brazil

Abstract -**The technological development of Global Positioning Systems (GPS) and the increase of its potential applications lead to the need of a channel simulation tool, in order to study different kinds of interference and attenuation in the GPS signal. The contribution of this work consists in the development of a software package that enables the analysis of error sources, as well as the environmental impacts on the GPS signal. We describe the developed simulator and analyze the effects of channel impairments in different scenarios, including urban, suburban, and rural environments. Multipath fading, Doppler effect, ionospheric and tropospheric delay, as well as antenna effects are studied for each scenario. The output data of the simulator is a digital file, which represents the signals issues from a GPS receiver in a selected environment.**

I. INTRODUCTION

GPS is a satellite system designed to provide worldwide position, velocity, and time information. The GPS system had a start point in the USA military applications, but it has been quickly employed to several tasks in civil and commercial areas, as transport, telecommunication, security and logistic.

In this way, the growing demand for GPS services points out the need of a signal simulator, including the effects that influence the performance of the receiver.

The channel simulator provides the observation of the effects of different error sources in several scenarios, thus enabling the comprehension of these effects, as well as how can this impair the results of GPS receiver localization. Figure 1 depicts the block diagram of the software package developed.

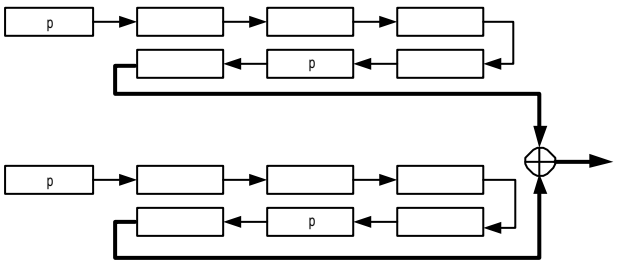

Sp = Spreading by C/A code; IE = Ionospheric effect; TE = Tropospheric effect; DS = Doppler-Shift; Sw = Shadowing; Mp = Multipath; ICN = Intentional Clock Noise

Fig. 1. Block Diagram

In the following, we provide a general explanation of Fig. 1. First of all, the signal crosses the atmosphere that is not a homogeneous media, thus introducing time delays due to the ionosphere and troposphere. Besides, the displacement of the satellite with respect to ground leads to a Doppler shift. As the signal arrives in the receiver, it undergoes several reflections due to the environmental or artificial obstacles, so multipath fading and shadowing are expected to occur. Power loss due to the propagation from the satellite as far as the ground, as well as intentional signal corruption associated with the injection of clock noise in the system by the GPS management center, also impairs.

The input data of our simulator is generated by another research group [1], that provides us with the complete GPS message, as well as with the relative GPS satellite position, that are visible for the receiver in a specific instant of time. After that, the distortion effects are added, and the user can observe each one separately or all effects together.

Next section describes the channel model with all characteristics to be considered in the simulator implementation. Section III gives an overview of the simulator structure while results for different scenarios are presented in Section IV. Finally conclusions are stated in Section V.

II. CHANNEL MODEL

Among the atmospheric effects on the GPS signal, we can observe the Faraday rotation. The right-hand circular polarization of GPS antennas minimizes the Faraday rotation, which may be ignored [2].

A. Ionosphere

The propagation of the GPS signal through ionosphere undergoes three major effects: attenuation, scintillation and delay.

The scintillation and attenuation effects are associated with the time-variant character of the ionospheric electronic content (TEC), leading to fluctuations in the GPS signal amplitude. They depend on the user position, hour, season and on the solar cycle.

The ionosphere also introduces a delay in the received GPS signal, which depends on the relative

user azimuth and elevation, with respect to the transmitting satellite.

Broadly speaking, scintillation may not impair the receiver for low-amplitude fluctuations, however this is not always true, specially for tropical regions and during high-solar activity periods. Since to our knowledge there is no closed-form modeling of scintillation specially suited for Brazil, and given the extreme time-variability of attenuation, these two effects were neglected as a first approach.

The model used to estimate the ionosphere delay is described in [3], and characterizes the average behavior of the ionosphere during quiet periods of solar activity. The following equations summarize the model.

$$T_{iono} = F \cdot \left[5.10^{-9} + (1 - \frac{x^2}{2} + \frac{x^4}{24}) \cdot \left(\sum_{n=0}^{3} a_n f_m^n \right) \right] \quad (1)$$

Where:

T_{iono} = ionospheric delay (seconds).

F = slant factor (seconds).

x = delay component, defined as below.

$$x = \frac{2p\,(t - 50400)}{\sum_{n=0}^{3} b_n f_m^n} \quad (2)$$

t = time at the receiver position (seconds).

β = GPS message coefficient beta (semicircles).

f_m = Receiver geomagnetic latitude (semicircles).

α = GPS message coefficient alfa (semicircles).

Of course, this does not cover all the situations, however to our knowledge there is no well-established method for estimating this delay during high solar activity. Figure 2 presents the delay for a typical situation of a fixed receiver, as a function of the elevation angle.

B. Troposphere

The troposphere also imposes attenuation and delay on the GPS signal. The attenuation may be neglected in view of the high amplitude of fading in the ground, according to [3]. The estimation of the delay is based on the Hopfield model, as presented below:

$$dtropo = \frac{Kd}{\left(\sin\left(\sqrt{E^2 + 1{,}904 \cdot 10^{-3}}\right)\right)} + \frac{Kw}{\left(\sin\left(\sqrt{E^2 + 0{,}6854 \cdot 10^{-3}}\right)\right)} \quad (3)$$

Where E is the elevation angle of the receiver (with respect to the satellite), Kd and Kw are respectively the delays associated with the dry and the wet layers of the troposphere. These delays depend on the air pressure and temperature.

Figure 3 presents the tropospheric delay for a typical situation.

C. Doppler Shift

Doppler shift is caused by the relative speed difference between a transmitter and a receiver. The change in the frequency depends on several parameters, such as the distance between the transmitter and the receiver, the speed of the electromagnetic waves, and their relative velocity.

For the receiver with constant speed v, moving in a certain direction that has the angle θ with the view line between receiver and transmitter, the frequency shift is:

$$f_d = \pm f_c \frac{v}{c} \cos q \quad (4)$$

Where f_c is the carrier frequency and c is the light speed. This expression does not take into account the relativistic effects and holds only for speeds lower than speed of the light.

In a GPS context, it is also necessary to consider that the Doppler shift depends on several other parameters, such as the altitude of the satellite, rotational speed of the Earth, and the elevation angle (from which the station is seen by the satellite). The frequency drift may be modeled by a differential equation as [4]:

$$\Delta f = \frac{1}{C} \frac{dD(t)}{dt} \quad (5)$$

Where the Δf is the Doppler frequency offset from the frequency f_c, C is the phase velocity of the light in the free space, and D(t) is a time function for the distance of the satellite and the Earth station.

D. Shadowing

Into the condition of no shadowing, the received signal can be expressed by the fasor sum of direct and diffuse components:

$$\vec{S}_{no\text{-}shadowing} = \vec{S}_{direct} + \vec{S}_{diffuse} \quad (6)$$

Partial shadowing is characterized by lots of small size obstacles disturbing the direct component, such as vegetation. In this case the transmitter has partial blocked view. As a consequence, attenuation decreases the power of the direct component and the spreading, causing deep fades which disturb the phase coherence. It is represented as:

$$\vec{S}_{direct\ partial\ shadowing} = A \cdot \vec{S}_{direct} + \vec{S}_{spread} \quad (7)$$

For total shadowing, there is no direct component and all received may be associated with the diffuse component:

$$\vec{S}_{shadowing} = \vec{S}_{diffuse} \quad (8)$$

E. Multipath

In this work, we consider the Clark model [5], where the incident field in the user is a set of N plane waves arriving in the direction of an azimuth plane, with arbitrary phases and arrival angles presenting the same amplitude average. It is considered that there is no line of sight incidence. The incident waves have an associated Doppler effect due to the user displacement and arrive in the receiver at the same time. Considering the transmission of a single tone in the carrier frequency, the n-th wave received by the user is thus given by:

$$\vec{E}_n = E_0 \cdot C_n \exp\{j[2p(f_c + f_n)t + f_n]\} \quad (9)$$

Where E_0 is the amplitude average close to the user, C_n is a random variable that represent the amplitude of

the n-th wave, f_c is the carrier frequency, f_n is the Doppler shift of the n-th wave and ϕ_n is a phase introduced by the reflector n. The phase ϕ_n depends on the material kind and on the reflection surface [6].

Using the central limit theorem and considering that N takes a big value, the components of the baseband wave are gaussian random variables with zero mean and variance given by $s_C^2 = s_S^2 = E_0^2/2$.

The channel amplitude gain is a random variable with Rayleigh distribution [7], according to the following expression.

$$p(r) = \frac{r}{s^2} \exp\left(-\frac{r^2}{2s^2}\right), \quad r \geq 0, \tag{10}$$

Where $s^2 = E_0^2/2$.

The phase response of the channel Φ(t) can be modeled as a random uniform variable in the interval $[0,2\pi)$.

The channel introduces different gain and frequency scattering due to different Doppler variations in each n-th ray. The received signal, as a result of one single tone, by a terminal that moves with constant speed can be represented as a carrier that has a random time-variant phase and amplitude.

F. Intentional Clock Noise

The signal degradation imposed by the GPS manager is modeled as an additive noise, which is added to the signal. At the same time, a Doppler shift is also included. The particular structure of the signal and the Doppler shift are established by the clock noise model, which is a stochastic process chosen from the following options:

- Gauss-Markov process of order 1
- Sinusoidal signal of random phase
- The signal in the output of a ARMA model driven by white-noise

The determination of the Doppler shift is based on the power spectrum of the clock noise model. So, after generating a random time series according to one of the three models presented above, we carry out the fast Fourier transform analysis and establish the Doppler shift as the component of higher energy. This component must lie within the ranges of the Doppler shift established by the models discussed in section 2.3 [8].

III. SIMULATOR STRUCTURE

The simulator structure is organized in order to consider spread spectrum of each visible satellite, by means of the satellite C/A code. Then the channel as could be seen in figure 1 disturbs these signals. The simulator also makes possible access the independent outputs to analyze each channel effect separately.

The signal is spread by a pseudorandom code (PN) [3] that is different for each satellite, and this allows the code division multiple access (CDMA) in the reception.

The multiplicative noise for each channel is obtained by the generation of a Rayleigh sequence that represents the diffuse component of the signal. This sequence is added with a lognormal parameters sequence (μ and σ) corresponding to the direct component times the attenuation factor.

The blocks Rayleigh and lognormal have as input the K_direct that is the power relation between the direct and diffuse component, and (μ and σ) for the lognormal sequence. The output is added to obtain a new sequence that corresponds to attenuation and phase rotation of the channel for each instant of time.

After that, the sequence undergoes Doppler effect, and it is multiplied in all instants by the satellite signals simulating this channel effects.

In order to simulate different kinds of environments, and knowing that their characterization are done by the presence or not of line of sight between satellite and receiver, and by obstacle density in the place, the Rayleigh and lognormal parameters are changed.

Here we choose working with three kinds of environments, rural, suburban and urban. The rural one is strong favorable to reception, because normally it has good line of sight between satellite and receiver; no obstruction in the direct component of the signal and the diffuse component is almost negligible.

In the urban one, there is almost not line of sight because of the presence of buildings, trees, and others; favoring the diffuse component with high density of spreaders.

The suburban one is between the two others; there is a shadowing line of sight and some spreads. This environment has a direct component with attenuation and a strong diffuse component.

The ionospheric and tropospheric blocks employ data from the incoming GPS message and equations presented above in order to estimate the delays, which must be converted from seconds into time samples. The last operation is carried out by supposing the sampling frequency of 4 x 1023 Mbits/s, according to [3]. Then the samples of the GPS signal are delayed according to the sum of the estimated delays.

IV. SIMULATIONS AND RESULTS

The results reported in the following consider three different towns (Las Vegas/USA, Manaus and Campinas/Brazil) and 8 visible satellites. The GPS receiver is supposed in a mobile platform (car) of constant speed of 100 km/h. All simulations consider an input signal transmitted during 30 seconds, including data updating at each 1.5 seconds. This transmission took place on February 18th 2002, beginning at 06h00 Brasília time. Two different multipath environments were considered: rural and urban. Simulations were carried out in a MATLAB environment, running on PCs.

Following the path presented in Fig. 1, the analysis of results begins with the ionospheric delay, depicted in Fig.2 as a function of the elevation angle. The parameters α and β were fixed during all the transmission, since significant changes in the TEC is not expected during the period of 30 seconds. From Fig. 2, one may conclude that the delay decreases as the elevation angle increases, and the variation associated

with the delay ranges approximately from 4 up to 14 ns.

Fig. 3 depicts the tropospheric delay as a function of the elevation angle. Similarly as for the ionospheric delay, the delay decreases as the elevation angle increases, and the variation associated with the delay ranges approximately from 10 up to 125 ns. Notice that these values are all higher than their respective ionospheric delays. In addition, the delays of Manaus are the highest ones, whereas the values associated with Las Vegas are the lowest, when the elevation angles are smaller than 20 degrees. This conclusion may be explained by the different physical characteristics of the troposphere over an equatorial region (Manaus) and over a North-hemispheric region (Las Vegas).

Fig. 4 presents the Doppler shift imposed on the received signal due to the relative movement of the receiver in respect of the satellite. Fig. 4 points out that the frequency drift ranges from -5 up to 5 kHz, which is imposed on the carrier frequency L1 = 1.57542 GHz.

Figs. 5 to 9 depicts the power spectral densities of several signals. Fig. 5 presents the signal just after the spread-spectrum, in the output of the satellite antenna, for one single satellite. Figs. 6 to 9 present the power spectral densities of the signal in the input of the GPS receiver, resulting from the sum of the particular signals associated with each satellite. Consequently, the input signal to the GPS receiver involves all distortions associated with the transmission. Particularly, Figs. 6 to 9 characterizes the specific physical phenomena associated with shadowing and multipath fading. Notice that the amplitudes of these figures consider the power loss due to wave propagation through the free-space between the satellite and the GPS receiver. The amplitudes are also set such that the average power of the signal attains the average standard value of –160 dBW [3].

Figs. 6 and 7 characterizes the propagation in a rural environment, and they should be compared to fig. 5. Notice that the envelope of the power spectral densities 5, 6 and 7 are very similar, pointing out that the direct signal component (line of sight) keeps up the signal spectral characteristics. These conclusions are in accordance of discussions of section IV.

Figs. 8 and 9 characterizes the propagation in an urban environment, and they should be compared to fig. 5. Notice that the envelope of the power spectral density of the transmitted signal (fig. 5) is significantly different from the envelopes of the power spectral densities of figs. 6 and 7. In fact, since the diffuse signal component takes significant values in this context, the GPS signal is spread, thus leading to a quite different power spectral density. At the same time, the attenuation of the direct signal component (line of sight) is very hard for the urban environment, thus leading to signal amplitude that is significantly lower as the amplitude in the case of the rural environment. This remark may be verified by comparing the amplitude of figs 6-7 (rural) to the amplitudes of figs. 8-9 (urban).

V. CONCLUSIONS AND PERSPECTIVES

In this paper we described the basic structure of the GPS channel simulator, discussing issues regarding the selection of models and choice of parameters to characterize atmospheric impairments. Simulations point out the capabilities of the simulator, which include a wide variety of environments, such as rural, urban users, as well as fixed or mobile receivers. It should be stressed that researchers on satellite communications may also employ the GPS simulator in general.

Future works involve further developments on the models of the physical phenomena, specially concerning ionospheric delay models well suited for the Latin American context [8], as well as scenarios involving new kinds of platforms carring GPS receivers (for instance, planes, rockets and satellites).

ACKNOWLEDGEMENTS

Special thanks are addressed to CNPq/RHAE program for funding this research project, as well as to several researchers who helped us during the development of this work. Among them we are particularly in debt with João Francisco Galera Monico and Benedito Márcio Furlan.

REFERENCES

[1] Furlan, B.M. *Simulation of the Constellation and the GPS Signal*; Technical Report, CNPq/RHAE project: Proc. 610062/99-9.

[2] Suh, S.-Y. and Stutzman, W. L. *A land mobile satellite communications propagation simulator*; Space Communications 15 (1998), pp. 33-53.

[3] Parkinson, B.W. and Spilker, J. J. *Global Positioning System: Theory and Applications, Volume I* J. J. Volume 163: Progress in Astronautics and Aeronautics, American Institute of Aeronautics and Astronautics

[4] Jamalipour; Abbas. *Low-Earth Orbital Satellite for Personal Communication Networks*, Artech House, 1997.

[5] Clarke, R. H. *A Statistical theory of mobile-radio reception*; Bell Systems Technical Journal, vol. 47 (1968), pp. 957-1000

[6] Rappaport, T. S. *Wireless Communications – Principles and Practice*; Prentice Hall (1996)

[7] Yacoub, M. D. *Foundations of Mobile Radio Engineering*; CRC Press (1993)

[8] Camargo, P.O *Ionospheric Regional Model for Single-Frequency Receivers Positioning*. PhD thesis, Federal University of Parana, Brazil, 1999 (in Portuguese).

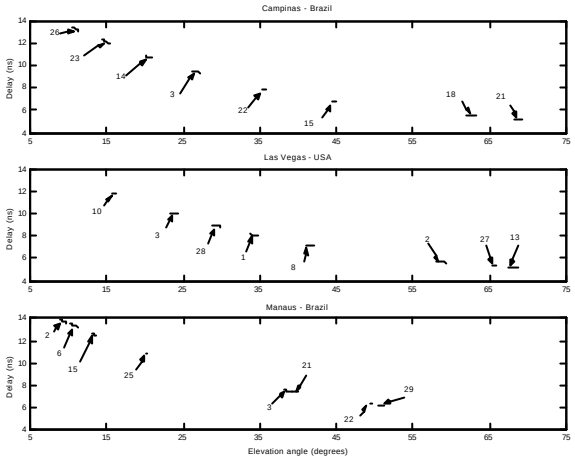

Figure 2 – Ionospheric delay as a function of the elevation angle

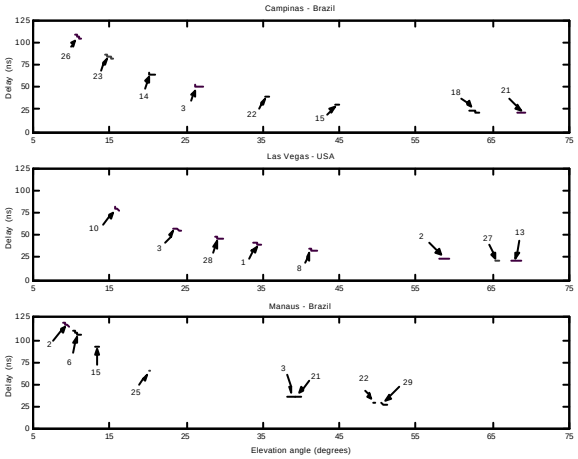

Figure 3 – Tropospheric delay as a function of the elevation angle

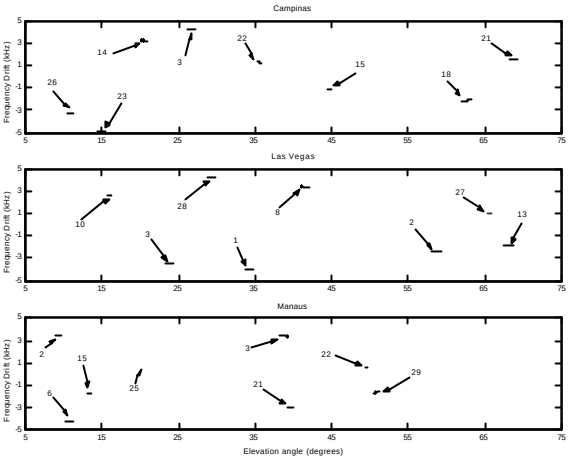

Figure 4 – Doppler Shift as a function of the elevation angle

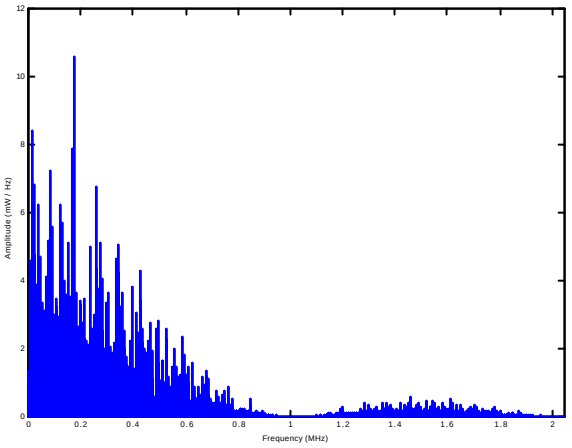

Figure 5 – Power Spectral Density of the signal generated for a satellite

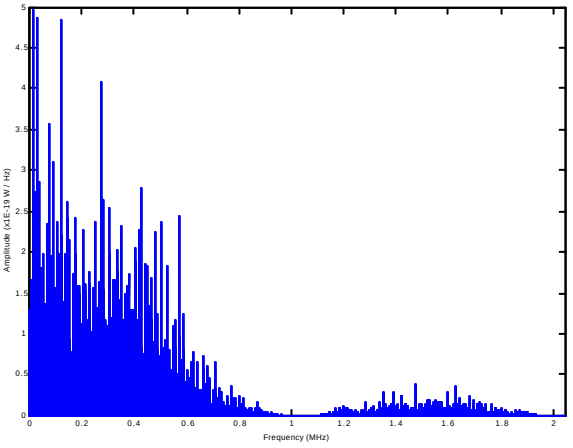

Figure 6 – Power Spectral Density of the received signal for a rural environment (Las Vegas – USA)

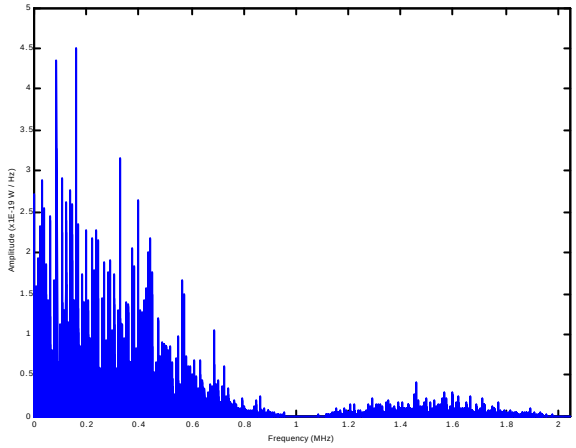

Figure 7 – Power Spectral Density of the received signal for a rural environment (Manaus – Brazil)

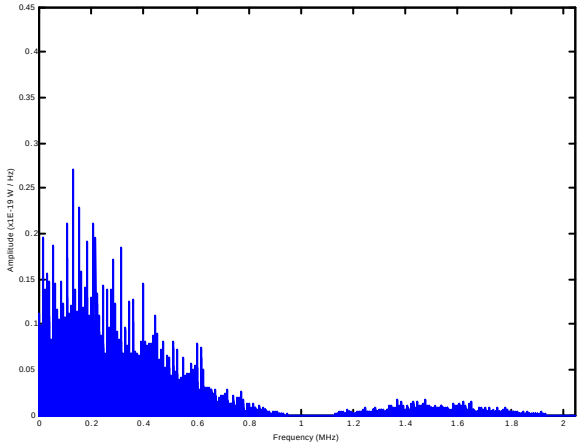

Figure 8 – Power Spectral Density of the received signal for an urban environment (Las Vegas – USA)

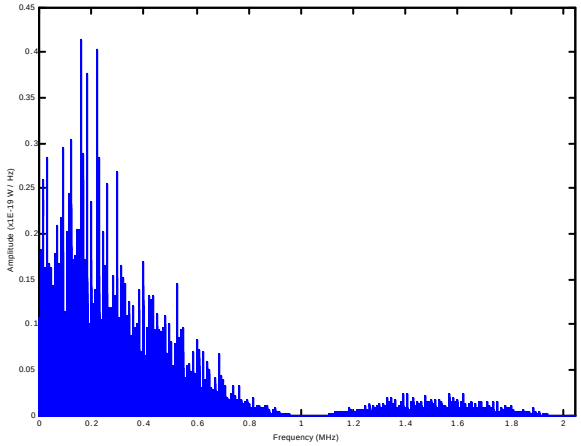

Figure 9 – Power Spectral Density of the received signal for an urban environment (Manaus – Brazil)